Industrial Crops and Products 52 (2014) 597–602

Contents lists available at ScienceDirect

Industrial Crops and Products

journal homepage: www.elsevier.com/locate/indcrop

Syngonanthus nitens: Why it looks like spun gold

L.S. Berlim[a], H.A. Gonçalves[a], V.S. de Oliveira[a], N. Mattoso[a], A.S. Prudente[b], A.G. Bezerra Jr.[c], W.H. Schreiner[a,*]

[a] Departamento de Física, Universidade Federal do Paraná, Centro Politécnico, Jardim das Américas, 81531-980 Curitiba, Paraná, Brazil
[b] Departamento de Farmacologia, Universidade Federal do Paraná, Centro Politécnico, Jardim das Américas, 81531-980 Curitiba, Paraná, Brazil
[c] Departamento Acadêmico de Física, Universidade Tecnológica Federal do Paraná Avenida Sete de Setembro, 3165, Centro, 80230-010 Curitiba, Paraná, Brazil

ARTICLE INFO

Article history:
Received 9 July 2013
Received in revised form 5 October 2013
Accepted 19 November 2013

Keywords:
Syngonanthus nitens
Flavonoids
Reflection

ABSTRACT

We report on the optical properties of *Syngonanthus nitens*, the golden grass, which is used to produce golden handicraft articles. The dry stems of the plant were analyzed with scanning electron microscopy, X-ray photoelectron spectroscopy, fluorescence microscopy; angle resolved optical reflectance and absorption/emission spectroscopy. The extract of the stems composed by 8 glucopyranosylflavones was also optically characterized. Electronic and geometric properties of the flavonoids were studied using ab initio and semi-empirical quantum mechanical calculations. The experimental and theoretical results explain the characteristic golden color of *S. nitens* dried stems.

© 2013 Elsevier B.V. All rights reserved.

1. Introduction

Syngonanthus nitens (Bong.) Ruhland is native to central Brazil and is called the golden grass due to its flower stem or scape which shines like spun gold, as shown in Fig. 1. Despite being erroneously called a grass, *S. nitens* is one of the more than six thousand species of the *Eriocaulaceae* (Schmidt et al., 2007) family. The stems are collected, dried and used as an important handicraft element, to produce golden decorative items, acquiring economical value and representing a real income for rural communities in certain Brazilian regions. Furthermore the decorative objects are sold and exported worldwide as exotic handcraftsmanship.

Scientific reports on *S. nitens* are rare in the literature and mainly devoted to economical/ecological sustainability aspects, and so it is surprising that its golden color origin has not been investigated. Exactly this particular color is the driving force to produce wealth with this crop.

2. Materials and methods: experimental

We used commercially available decorative golden grass samples for this study. The stems were cut to adequate pieces for the different characterizations. The extracts were obtained suspending the scapes in methyl alcohol or distilled water at room temperature and ultrasonicating for 1 h.

SEM (Scanning Electron Microscopy) images of the scapes were obtained using a VEGA3 TESCAN operating at 30 kV. The 3D, roughness and waviness results were obtained using three scans (sample normal, +5° and −5°) of the same selected area employing ALICONA MeX software.

XPS (X-ray photoelectron spectroscopy) measurements were done using a VG Microtech ESCA 300 system with an Al X-ray anode, a 250 mm semi-hemispherical energy analyzer, 9 channeltron detectors and a base vacuum of 3×10^{-10} mbar. The energy resolution of the system was of 0.8 eV. Quantification of the elements on the sample surface was done using the systems proprietary software.

The fluorescence microscopy was done on an Olympus DX51 with detector DP72 using the following Olympus filters: U-MWU2, U-MWB2, U-MWG2, U-N31004, U-N31005, and U-M00050.

The UV–vis reflection spectra of the stems and the absorption/transmission spectra of the extract suspension were obtained with an Ocean Optics USB2000 spectrometer.

The fluorescence measurements were done on a Shimadzu spectrofluorophotometer model RF-5301 PC.

For the angle resolved reflectance measurements a homemade goniometer was used, employing RGB (Red Green Blue) laser diodes operating at 650, 532 and 405 nm, respectively, and the above mentioned Ocean Optics spectrometer. For these measurements the stems were fixed on a planar substrate with adhesive.

* Corresponding author. Tel.: +55 41 33613427.
E-mail address: wido@fisica.ufpr.br (W.H. Schreiner).

0926-6690/$ – see front matter © 2013 Elsevier B.V. All rights reserved.
http://dx.doi.org/10.1016/j.indcrop.2013.11.030

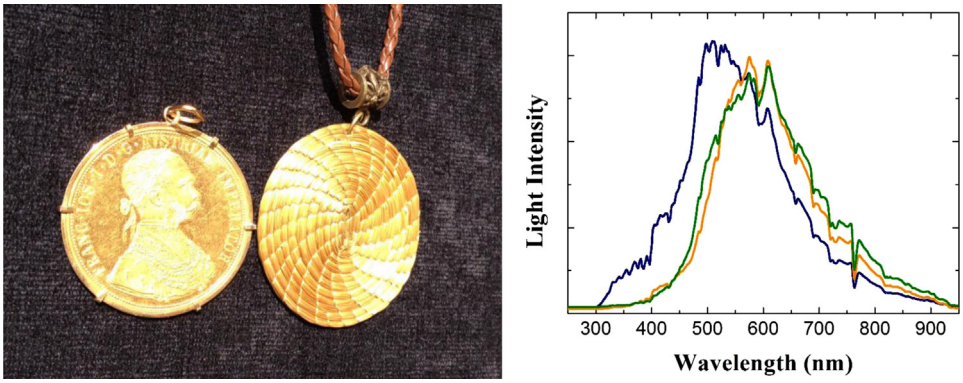

Fig. 1. A comparison of the visual appearance of a gold coin and *S. nitens* handicraft. The resemblance of both objects is also shown by reflectance measurements of sunlight (right). The solar spectrum (blue line) was directly taken by an optical fiber attached to the spectrometer. Light reflection was collected at 45° for gold (yellow line) and *S. nitens* (green line).

3. Materials and methods: theoretical

Electronic and geometric properties of flavonoids were studied using *ab initio* quantum mechanical calculations. First, the geometry of each flavonoid was optimized with the DFT (Density Functional Theory) method using the Becke three-parameter, (Lee–Yang–Parr functional B3LYP, 1988) which is a hybrid functional of exact (Hartree–Fock) exchange with local and gradient-corrected exchanges and correlation terms used in calculations of very large molecules (Stephens et al., 1994). A set of Gaussian Split-based Valence wave function basis was used (Frisch et al., 2009). For purposes of reliability in the calculations, the geometry was previously optimized using the basic Gaussian split-valence (with double diffuse functions) 6-31G(d,p) basis, which gives good ground state geometries for conjugated polymers (Hsu et al., 2010; Lin et al., 2003). These simulations were performed using the GAUSSIAN 09 package (Frisch et al., 2009). DFT/B3LYP calculations with the 6-31G(d,p) basis set running GAUSSIAN 09 were performed.

Finally, simulation of the optical absorption spectrum of flavonoid immersed in a methanol solution and water solution were performed using ZINDO (Zerner's intermediate neglect of differential overlap/single) (Frisch et al., 2009) running under the GAUSSIAN 09 program. The optical absorption spectra were calculated with PCM (Polarizable Continuum Model) (Frisch et al., 2009) using the integral equation formalism variant SCRF (Self-Consistent Reaction Field) solvation models, for 60 excited states. The ZINDO transition energies were weighted by the oscillator strength values.

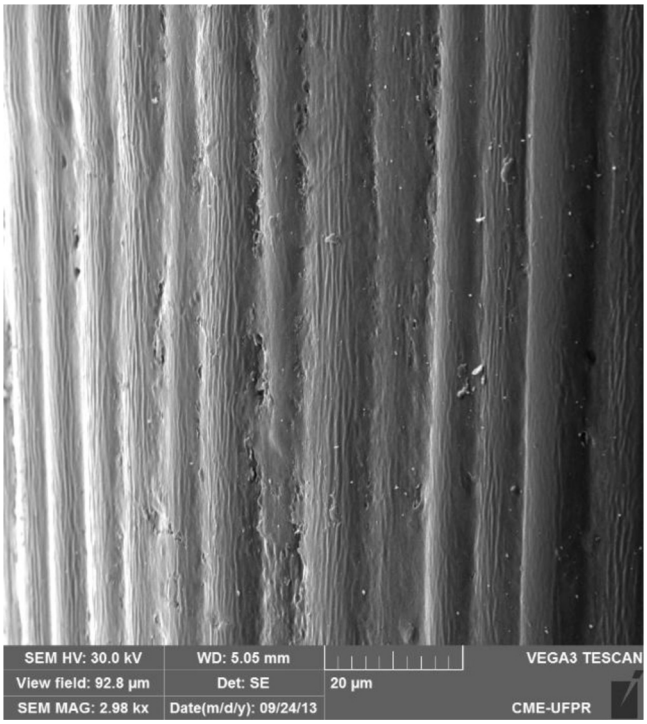

Fig. 2. Scanning electron microscope image of the *S. nitens* stem surface. The surface is characterized by a micro/nano-structure which runs along the stem axis. The SEM magnification for this image was 2.98 kX.

4. Results

The first aspect studied for the characterization of *S. nitens* stems was their elemental surface composition. A quantification via XPS spectra led to C 86.6 at%, O 11.7 at% and with Si 1.7 at% as the single impurity. The high carbon content of at the surface is due to the epidermis of the stems (Scatena et al., 2004), which is composed mainly by cutin, waxes, C24 and C34 alkanes (Javelle et al., 2004).

Other elements, specifically metals, were not found (H is not measured by XPS), showing that the golden color is not due to some extraneous element or elements.

Recently (Siqueira et al., 2010), while trying to reinforce natural rubber with *S. nitens* fibers, determined the composition of the biological material which constitutes the golden scapes. They found that the stems are formed by 90% (w/w) holocellulose (67% cellulose and 27% hemicelluloses), 6.5% (w/w) lignin, 1.2% (w/w) ashes and 0.75% (w/w) extractives. The cellulose crystallinity index of the scales was found to be about 70.1%. Thus, the stems have high cellulose content, almost as high as cotton lint (Satyanarayana et al., 2007). Thus, also here only organic materials were found.

The scanning electron microscopy images of *S. nitens* stems, shown in Fig. 2, clearly indicate rather smooth surfaces with a ~10 μm waviness. Within those undulations several smaller grating-like nanostructures are seen. The overall surface smoothness is responsible for the shiny aspect of the stem surface, as it is common for polished materials.

A 3D image of a selected area of 47 × 35 μm^2 of the stem surface is shown in Fig. 3. The waviness and the roughness graphs of a virtual line scan on this 3D image are also shown in Fig. 3. The typical waviness periodicity is of 10 ± 1 μm and the mean roughness is of 98 ± 3 nm, while the roots mean square (RMS) roughness is of 128 ± 3 nm.

These data are obtained only of one image and therefore are only an indication of the general topography of the stem surface. Nevertheless they are sufficient to rule out visible light interference

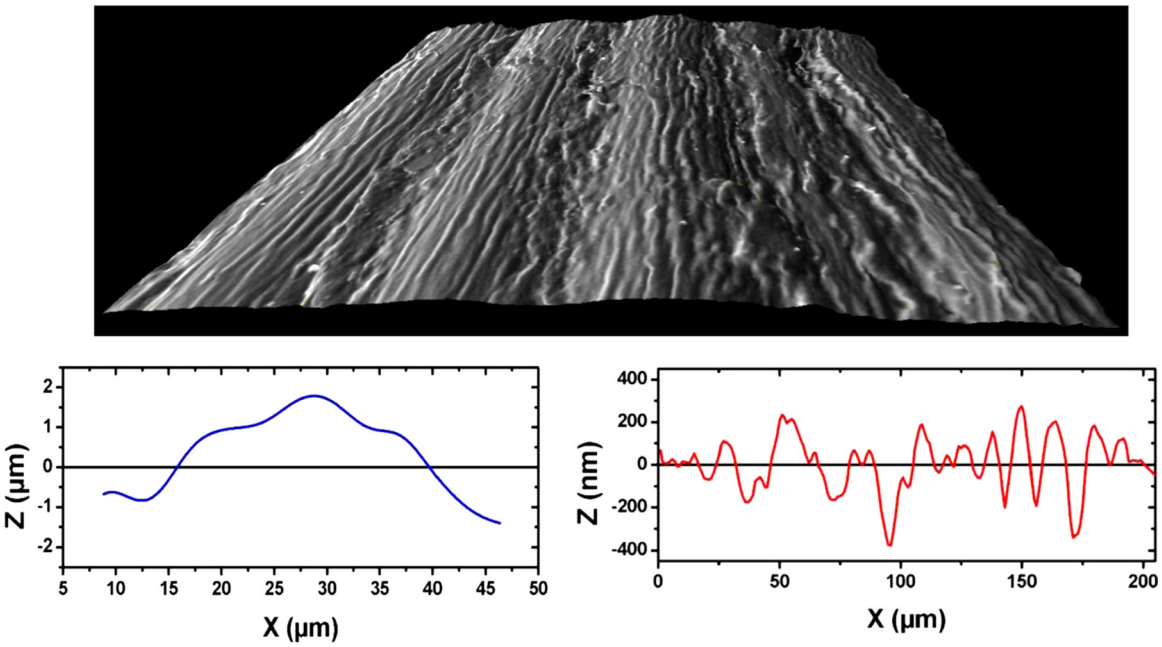

Fig. 3. 3D image and typical waviness (below left) and roughness (below right) of the *S. nitens* surface.

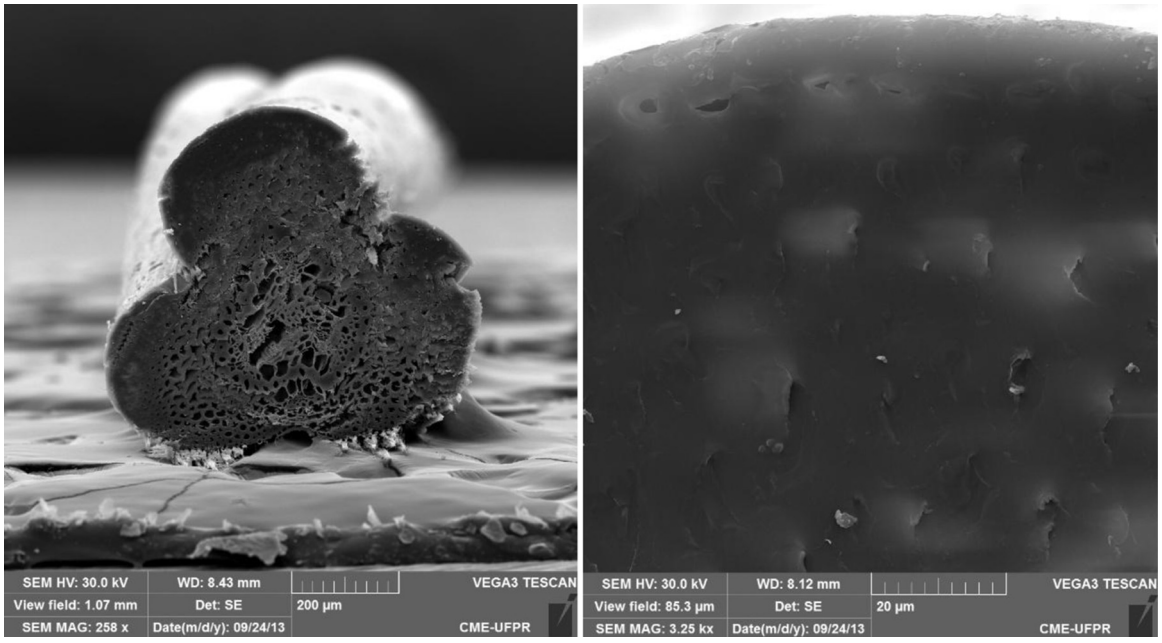

Fig. 4. Cross-sectional SEM images of a *S. nitens* stem. The magnification was, respectively, of 258 X (left) and 3.25 kX (right).

effects, since the features are either far above or far below the visible light wavelength.

The SEM surface characterization per se is not sufficient to rule out an underlying structure. Thus a cross-sectional analysis was mandatory, and the resulting images are shown in Fig. 4.

The dry stems have a peculiar three-lobed arrangement with the xylem and phloem channels far away from the epidermis. The amplified image at the left of Fig. 4 shows a very compact structure starting right below the epidermis. This finding rules out structure related light interference and iridescence.

Additionally, we measured angle resolved light reflection (not shown). The results show that the three RGB wavelengths reflect nearly specularly, while the blue reflectance spectra show clear but weak fluorescence components. No grating interference or diffraction effects could be detected. This result together with the SEM imaging ruled out surface or near surface structuring as the possible cause of the golden aspect of the scapes.

The stem fluorescence, detected by the reflectance measurements, was further analyzed, by observing the scapes under a fluorescence microscope.

Fig. 5 shows a series of images of the scales illuminated under different wavelengths with several excitation and emission filters. The stems fluorescence is stimulated by a very broad range of wavelengths, starting under ultraviolet excitation up to larger wavelengths.

Having found no surface structure related effects the study concentrated on the organic components besides cellulose and lignin which are present at the stem surface.

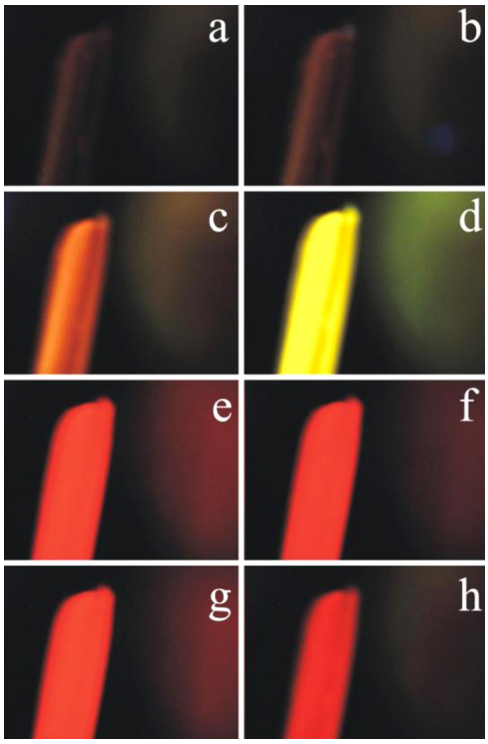

Fig. 5. Fluorescence images of a *S. nitens* stem obtained with different wavelength excitation illuminations and fluorescence filters. The stem surface fluoresces at all wavelengths, from UV (a) to red (h).

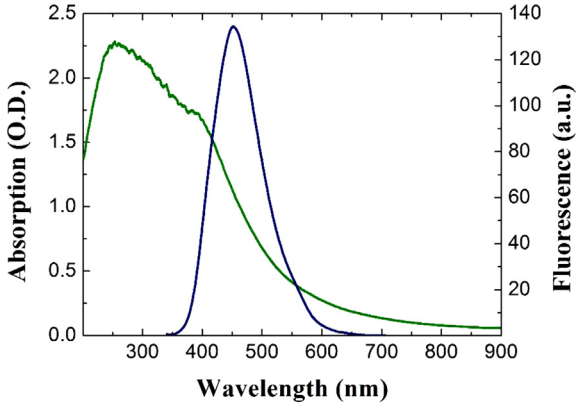

Fig. 6. Absorption spectrum of *S. nitens* extractives in water (in green) and fluorescence spectrum (in blue) of the same suspension upon excitation at 325 nm. (For interpretation of the references to color in figure legend, the reader is referred to the web version of the article.)

Fig. 6 shows absorption and fluorescence emission spectra of *S. nitens* extracts in water. The suspension absorbs high frequency light, mainly from the UV to green and fluoresces in the greenish/red range. This broad fluorescence emission, centered at 470 nm, is obtained when the suspension is excited at different wavelengths (between 225 nm and 375 nm). Thus, the extracts are able to absorb short wavelengths and emit at long wavelengths with large Stokes shifts.

Trying to understand these absorption characteristics of the extracts from a theoretical point of view, several molecules found in the *S. nitens* extract, as described in detail by Pacifico et al. (2011), were used. These molecules were identified by those authors as flavonoids. They found 8 molecules, 5 flavones and 3 flavanones. Their numbering and identification are as follows:

3′,4′,5,-tetrahydroxy-6-C-glucopyranosylflavone
3′,4′,5,-trihydroxy-7-methoxy-6-C-glucopyranosylflavone
5- 3′,4′,5,-trihydroxy-7-methoxy-6-C-glucopyranosylflavanone
7- 3′,4′,5,-trihydroxy-7-methoxy-8-C-glucopyranosylflavone
8- 4′,5,-dihydroxy-3′,7-dimethoxy-6-C-glucopyranosylflavone
9- 3′,4′,5,-trihydroxy-7-methoxy-8-C-glucopyranosylflavanone
10- 4′,5,7-trihydroxy-8-C-glucopyranosylflavanone
17- 3′,4′,5,7-tetrahydroxyflavone

Fig. 7 shows the optimized geometry of 2 representative species of the 8 molecules which were found in the *S. nitens* stems extracts. The figure also shows the calculated ground state HOMO (highest occupied molecular orbital) and the excited LUMO (lowest unoccupied molecular orbital) electron density, respectively at the center and at the right of the figure for the two flavonoids. The other remnant 6 molecules were calculated but are not shown here.

The theoretical absorption spectra of electrons transitioning between ground and excited states obtained from those simulations are shown for all 8 molecules in Fig. 8. Two groups are found. All flavonoids have strong oscillator strengths in the UV region and the flavones 1, 3, 7, 8 and 17 have additionally a significant oscillator strength component toward the blue region of the spectrum. Thus, the flavonoid mixture should absorb light from roughly 200 to 450 nm, according to this theoretical simulation.

Fig. 9 shows a solar spectrum (blue), taken noon 09/14/2012 outside our labs, together with the transmission spectrum of *S. nitens* extractives (black). In green we show the reflectance spectrum of the scapes for sunlight reflected at 45 degrees, obtained at the same date and location. In yellow we show the (blue) solar spectrum multiplied by the (black) absorption spectrum of the extracts. The yellow and green spectra were normalized to the same intensity. The red shift obtained for the resulting yellow spectrum compared to white light is indeed remarkable. Noteworthy is also the superposition of the yellow (calculated) and green (experimental) spectrum.

5. Discussion

S. nitens is native in certain areas of central Brazil and is one of the more than six thousand species of the *Eriocaulaceae* (Schmidt et al., 2007) family.

The typical golden aspect of the dried stems has to originate from the peculiar interaction of white light with the stem surface.

When considering bulk metallic gold, the conduction electrons are essentially free, moving relatively unimpeded through the lattice. Damping effects arise due to collisions of these electrons with lattice imperfections. The reflectivity of metals is caused by the interaction of those free electrons with the incident electromagnetic field. At frequencies corresponding to visible light, the penetration depth is minimal, and light is almost entirely reflected. This gives metals its shiny aspect (Jackson, 1998). In addition, for gold, there occur electron excitations from the 5d band, which is very near to the Fermi edge. These excitations are caused by the absorption of photons in the violet/blue range of the visible spectrum and the reflection of white light shows the typical red coloring of this precious metal (Takata et al., 2004). Our XPS measurements show that no metallic element was found on the golden grass surface.

Several species in fauna, on the other hand, are capable of producing bright golden colors due to surface structures and patterns.

Coleoptera, for example, present golden iridescence based on multilayer reflectors on their elytra (Vigneron et al., 2005; Seago et al., 2009). Butterflies display iridescent colors due to cuticles and lamellae held apart by air layers (Vigneron and Simonis, 2012). Jeweled beetles, like the *Chrysina aurigans*, display

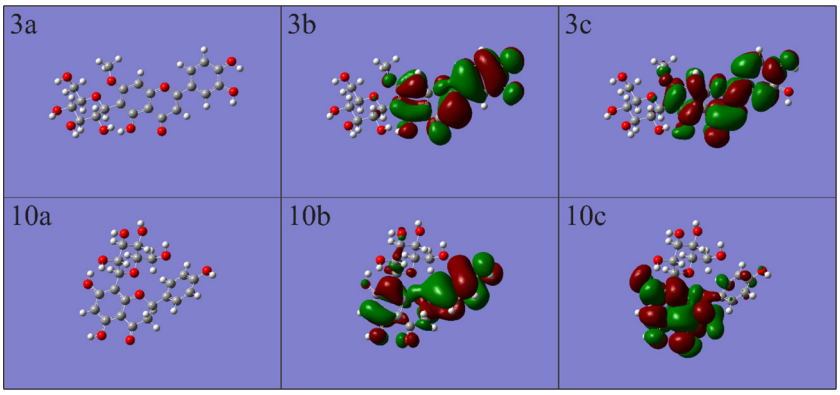

Fig. 7. Optimized geometry of flavonoids 3 and 10 (left) (see the numbering described in the text) with their respective HOMO (middle) and LUMO (right) molecular orbital electron density.

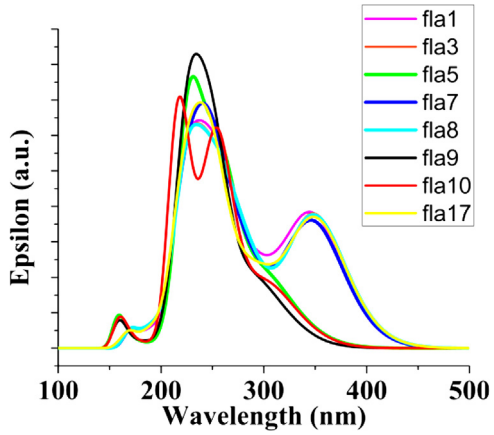

Fig. 8. Theoretically calculated absorption spectra for the 8 flavonoids found and described earlier by Pacifico et al. (2011)(see numbering and identification of the flavonoids in the text).

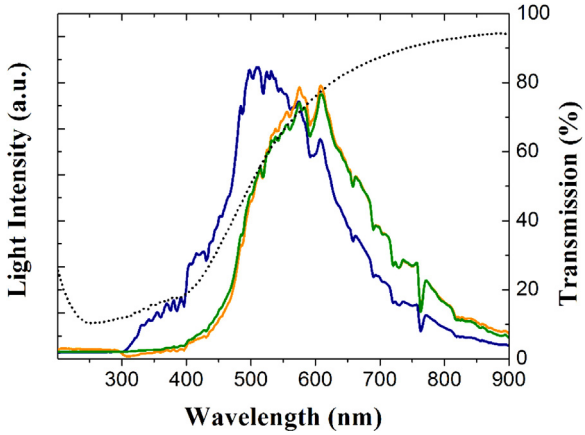

Fig. 9. The four spectra shown are: the solar spectrum on a sunny day in southern Brazil (blue line); the transmission spectrum of *S. nitens* extractives (dotted black line); the experimental reflectance spectrum of *S. nitens* (green line); and the resulting curve (yellow) after multiplication of the solar spectrum by the transmission spectrum.

iridescence through circularly polarized light reflectance from surface structures, similar to cholesteric liquid crystals (Sharma et al., 2009). Iridescence effects in flora are less frequent, but surface photonic structures have been identified in *Leontopodium nivale* subsp. *Alpinum* (Vigneron et al., 2005), in the *Pollia condensata* fruit (Vignolini et al., 2012a) and in the *Ophrys speculum* the mirror orchid flower (Vignolini et al., 2012b). These surface structures were not found for *S. nitens* stems, as clearly shown by our SEM images.

Fortunately, for our purposes, *S. nitens* extracts were analyzed recently in great detail by Pacifico et al. (2011). Their report shows that the extractives (organic molecules which are present in the stems besides cellulose and lignin) are composed mainly by a series of flavonoid derivatives. They extracted 17 different flavonoids of flowers and stems, 6 of them being unambiguously classified as unknown new molecules. The stem extracts could be associated to 8flavonoids, 6 known and 2 new molecules. They guessed, without the support of further experiments, discussions or data, that those flavonoids could reasonably be considered responsible for the scapes' golden color.

Flavonoids in plants are well described in the literature. They contribute to the color of flowers and are well known to act as UV filters in leaves. Additionally, these molecules have shown antibacterial and antifungal properties, defending plants from diseases. Those peculiar qualities led to research on pharmacological benefits of flavonoids for humans. On another note, flavonoid presence in plants can also deter mammalian herbivores from eating their leaves. By 1999 more than six thousand flavonoid species were known (Harborne and Williams, 2000).

Our theoretical absorption calculations of these flavonoids (Fig. 8) show that indeed these molecules are capable to absorb UV, violet and blue. The absorption centered at 350 nm extending up to 450 nm is most important, since a significant part of the solar spectrum near the earth's surface is found in this range. This result also explains the UV absorption of flavonoids as described in the literature (Harborne and Williams, 2000). Good agreement of the theoretical calculations with the experimental absorption results of *S. nitens* extracts is also noted.

6. Conclusion

We come to conclude that the golden color of dry *S. nitens* stems is caused by the interaction of incident light with the several flavonoids present at the surface epidermis of the dry scapes. Upon reflection at the smooth stem surface, a substantial part, mainly in the high frequency range of the incident light, is absorbed due to the flavonoid presence and not reflected. Therefore, light reflection produces a shift in the solar spectrum peak toward longer wavelengths. In addition, the flavonoids are shown to fluoresce in the longer wavelength range, which also contributes to the red shift.

In this sense, the solar spectrum should be multiplied by the flavonoid's extract transmission curve to yield the resulting reflectance spectrum. The latter is plotted together with the

measured reflectance spectrum in Fig. 9, indicating a very good agreement in support to our hypothesis. These optical properties give *S. nitens* its exquisite reddish golden aspect mimicking spun gold.

Together with conduction electrons (in metals), and interference effects due to surface structures (e.g. some butterflies and beetles), it seems that nature has also found another peculiar way of producing brilliant metallic brightness, based on a quite ingenious combination of surface geometry (smoothness) and light absorption, as we demonstrate here for *S. nitens*, the golden grass.

Acknowledgements

The authors thank CNPq – Conselho de Desenvolvimento Científico e Tecnológico, a Brazilian science fostering agency, for scholarships and financial support

References

Frisch, M.J., 2009. Gaussian 09, Revision B.01. Gaussian Inc., Wallingford, CT.
Harborne, J.B., Williams, C.A., 2000. Advances in flavonoid research since 1992. Phytochemistry 55, 481–504.
Hsu, S.L., Chen, C.M., Wei, K.H.J., 2010. Carbazole-based conjugated polymers incorporating push/pull organic dyes: synthesis, characterization and photovoltaic applications. Polym. Sci. A: Polym. Chem. 48, 5126–5134.
Javelle, M., Vernoud, V., Rogowsky, V.P.M., Ingram, G.C., 2004. Epidermis: the formation and functions of a fundamental plant tissue. New Phytol. 189, 17–39.
Lee, C., Yang, W., Parr, R.G., 1988. Development of the Colle–Salvetti correlation energy formula into a functional of the electron density. Phys. Rev. B 37, 785–789.
Lin, B.C., Cheng, C.P., Lao, Z.P.M., 2003. Reorganization energies in the transport of holes and electrons in organic amines inorganic electroluminescence studied by density functional theory. J. Phys. Chem. A 107, 5241–5252.
Scatena, V.L., Vich, D.V., Parra, L.R., 2004. Anatomia de escapos, folhas e brácteas de *Sygonanthus sect* Eulapis (Bong. ex Koern.) Ruhland (*Eriocaulaceae*). Acta Bot. Bras. 18, 825–837.
Pacifico, M., Napolitano, A., Masullo, M., Hilario, F., Vilegas, W., Piacente, S., dos Santos, L.C., 2011. Metabolite fingerprint of capim dourado (*Syngonanthus nitens*), a basis of Brazilian handcrafts. Ind. Crops Prod. 33, 488–496 (2011).
Jackson, J.D., 1998. Classical Electrodynamics, third ed. J. Wiley & Sons, Hoboken, NJ.
Satyanarayana, K.G., Guimaraes, J.L., Wypych, F., 2007. Studies on lignocellulosic fibers of Brazil. Part I: Source, production, morphology, properties and applications. Composites A: Appl. Sci. Manufact. 38, 1694–1709.
Schmidt, I.B., Figueiredo, I.B., Scariot, A., 2007. Ethnobotany and effects of harvesting on the population ecology of *Singonanthus nitens* (Bong.) Ruhland (*Eriocaulaceae*), a non-timber forest product from Jalapão region, central Brazil. Econ. Bot. 61, 73–85.
Seago, A.E., Brady, P., Vigneron, J.P., Schultz, T.D., 2009. Gold bugs and beyond: a review of iridescence and structural color mechanisms in beetles (*Coleoptera*). J. R. Soc. Interface 6, S165–S184.
Sharma, V., Crne, M., Park, J.O., Shrinivasarao, M., 2009. Structural origin of circularly polarized iridescence in jeweled beetles. Science 325, 449–451.
Siqueira, G., Abdillahi, H., Bras, J., Dufresne, A., 2010. High reinforcing capability cellulose nanocrystals extracted from *Syngonanthus nitens* (*Capim Dourado*). Cellulose 17, 289–298.
Stephens, P.J., Devlin, F.J., Chabalowski, C.F., Frisch, M.J.J., 1994. Ab initio calculation of vibrational absorption and circular dichroism spectra using density functional force fields. Phys. Chem. 98, 11623–11627.
Takata, Y., Tamasaku, K., Tokushima, T., Miwa, D., Shin, S., Ishikawa, T., 2004. A probe of intrinsic valence band electronic structure: hard X-ray photoemission. Appl. Phys. Lett. 84, 4310–4312.
Vigneron, J.P., Rassart, M., Vértesy, Z., Kertész, K., Sarrazin, M., Biró, L.P., Ertz, D., Lousse, V., 2005. Optical properties and function of the white filamentary hair covering the edelweiss bracts. Phys. Rev. E 71, 011906–011908.
Vigneron, J.P., Simonis, P., 2012. Natural photonic crystals. Physica B 407, 4032–4036.
Vignolini, S., Rudall, P., Rowland, A.V., Reed, A., Moyroud, E., Faden, R.B., Baumberg, J.J., Glover, B.J., Steiner, U., 2012a. Pointillist structural color in Pollia Fruit. PNAS 109, 15712–15715.
Vignolini, S., Davey, M.P., Bateman, R.M., Rudall, P.J., Moyroud, E., Tratt, J., Malmgreen, S., Steiner, U., Glover, B.J., 2012b. The mirror crack'd: both pigment and structure contribute to the glossy blue appearance of the mirror orchid, *Ophrys speculum*. New Phytol. 196, 1038–1047.